Long-distance corticocortical GABAergic neurons in the adult monkey white and gray matter

Journal:	*The Journal of Comparative Neurology*
Manuscript ID:	JCN-07-0065.R3
Wiley - Manuscript type:	Research Article
Keywords:	EGFP-adenovirus, interstitial neuron , muscarinic receptor, neuronal NOS, non-pyramidal neuron, somatostatin

Long-distance corticocortical GABAergic neurons in the adult monkey white and gray matter

RYOHEI TOMIOKA[1*] and KATHLEEN S. ROCKLAND[1, 2,]

[1]Lab for Cortical Organization and Systematics, RIKEN Brain Science Institute, Wako-shi, Saitama 351-0198, Japan.

[2]Graduate School of Science and Engineering, Saitama University, Saitama-shi, Saitama 338-8570, Japan

Abbreviated Title: GABAergic projection neurons in monkey cortex

Associate Editor: Dr. Joseph L. Price

Key Words: EGFP-adenovirus, interstitial neuron, muscarinic receptor, neuronal NOS, non-pyramidal neuron, somatostatin

*Correspondence to: Dr. Ryohei Tomioka
Lab for Cortical Organization and Systematics
RIKEN Brain Science Institute
2-1 Hirosawa, Wako-shi, Saitama 351-0198, Japan
Telephone: +81.48.467.6427
Fax: +81.48.467.6420
Email: rtomioka@brain.riken.jp

Supporting Grant: We gratefully acknowledge research funding from RIKEN Brain Science Institute.

Abstract

A subgroup of GABAergic neurons has been reported to project over long distances in several species. Here, we demonstrate that long-distance cortically projecting non-pyramidal neurons occur in monkeys in both white and gray matter. Non-pyramidal neurons were first identified morphologically. Visualization of Golgi-like details was achieved by retrograde infection from injections of an adenovirus vector, producing enhanced green fluorescent protein (EGFP) under control of a neuron-specific promoter. Injections in areas V1, V4, TEO, and posterior TE resulted in EGFP-expressing non-pyramidal neurons up to 1.5 cm distant from the injections, mainly in the white matter. Some neurons occurred in the gray matter, mainly in layer 3, but also in layers 5 and 6, and, very occasionally, layer 1. As control, we injected cholera toxin subunit B, a standard retrograde tracer, in V4, and observed a similarly wide distribution of neurons in the white matter. Secondly, the GABAergic identity of EGFP-expressing non-pyramidal neurons was established by co-labeling for EGFP and GAD67 in selected tissue sections. Most neurons positive for EGFP and GAD67 were positive for somatostatin (SS; 90%). Of those neurons positive for EGFP and SS, almost all were also positive for neuronal nitric oxide synthase or m2 muscarinic receptor, but only 23% were also positive for calretinin. None were positive for parvalbumin. We conclude that long-distance projecting GABAergic neurons 1) are phylogenetically conserved, although in monkeys, most gray matter neurons are in the upper layers, and 2) are heterogeneous in terms of their neurochemistry, location, and potentially function.

Introduction

The overwhelming majority of long-distance connections in the cerebral cortex originate from glutamatergic pyramidal neurons. These make about 80% of their terminations onto other pyramidal neurons and 20% onto inhibitory interneurons, the source of important inhibitory effects (DeFelipe and Farinas, 1992). Several investigations in rodents and carnivores, however, have provided evidence that a small number of inhibitory non-pyramidal neurons, mainly in the deeper cortical layers and white matter, have long-distance ipsi- or contralateral connections. These findings are based on various techniques: double labeling by GABA-immunocytochemistry and retrograde tracers (Peters et al., 1990; McDonald and Burkhalter, 1993; Gonchar et al., 1995; Fabri and Manzoni, 1996, 2004; Jinno and Kosaka, 2004; Higo et al., 2007), double labeling by the retrograde fluorescent tracer in GAD67-GFP knock-in mice (Tomioka et al., 2005), and double labeling for PHA-L and GABA, with electron microscopic inspection (Pinto et al., 2006).

Long-distance projecting non-pyramidal neurons have been demonstrated to make synaptic contacts (Clancy et al., 2001), and their function has been discussed in the context of receptive field properties (Peters et al., 1990; Clancy et al., 2001) or synchronization (Buzsaki, 2006). So far, however, much less information is available concerning long-distance projecting non-pyramidal neurons specifically in primates. That is, white matter (or "interstitial") neurons are known to exist in primates as in other species (Kostovic and Rakic, 1980, 1990; Smiley et al., 1998), but there are no reports concerning their projections. The white matter population of GABAergic neurons is widely dispersed and difficult to target for connectivity studies, especially in larger

brains.

In this communication, we demonstrate that a subpopulation of non-pyramidal neurons in the macaque monkey has long-distance ipsilateral cortical connections. These neurons are scattered in both the gray and white matter. They were initially identified as non-pyramidal by morphological criteria. In particular, there was no obvious apical dendrite and dendritic spines were either lacking or sparsely distributed (Peters and Jones, 1984). These features could be easily assessed owing to the detailed, Golgi-like labeling produced by infection with an adenovirus vector for EGFP-expression. The virus vector was retrogradely transported subsequent to intracortical injections (Tomioka and Rockland, 2006). Subsequently, we confirmed that neurons identified as non-pyramidal were GABAergic in selected sections, where we directly ascertained co-labeling for EGFP and GAD67 (DeFelipe, 1997; Gonzalez-Albo et al., 2001).

Materials and Methods

Preparation of recombinant adenovirus vector

The adenoviral vector is based on human adenovirus type 5, and is replication incompetent because it lacks the E1 and E3 regions of its genome. The adenoviral (Ad) vector expresses EGFP under the control of a neuron-specific promoter synapsin I (Syn), as described previously (Tomioka and Rockland, 2006). The AdSynEGFP was purified and concentrated by double cesium step gradient centrifugation and dialyzed in 50 mM Tris-HCl (pH8.1) containing 600 mM NaCl. The viral suspensions were stored at 4°C for up to 1 month after the date of purification. The titers of viral stocks were determined by plaque assay on HEK 293 cells and adjusted to more than 1.0 x 10^{12} pfu/ml before the injection.

Producing anti-EGFP antibody

Antibodies against EGFP were produced in rabbits (see Tomioka and Rockland, 2006 for full details), and in guinea pigs. In general, antibody production in guinea pigs is the same as in rabbit. Briefly, the purified EGFP was emulsified with Freund's Complete Adjuvant (Difco, Detroit, MI), and injected intracutaneously into four female guinea pigs (0.5 mg/animal). Three weeks after the first immunization, the same amount of EGFP emulsified with Freund's Complete Adjuvant was re-injected into the guinea pigs. Additional immunizations were performed every two weeks thereafter. After the 3rd immunization, serum was taken from the guinea pigs. Antibodies were affinity-purified with EGFP-conjugated Affigel 10 gel (BioRad, Richmond, CA; 2 mg EGFP/1 ml gel). Crude-globulin fraction (25 mg) was applied to 1 ml of the antigen column; and the specific antibody was eluted with 0.1 M glycine-HCl (pH 2.5) and mixed with 1 M

potassium phosphate buffer (10:1) to achieve neutral pH. The antibody was stored at 4°C with 0.02% NaN_3.

Animals and tracer injection

Seven adult macaque monkeys (*Macaca mulatta* and *Macaca fuscata*) were used in this study. Experimental protocols were approved by the Safety Division of the RIKEN Institute, and were carried out in biosafety level 2 rooms in accordance with the USA NIH Guidelines for Research Involving Recombinant DNA Molecules. All experimental animal protocols were approved by the Experimental Animal Committee of the RIKEN Institute. Surgery was carried out under sterile conditions after the animals were deeply anesthetized with barbiturate anesthesia (35 mg/kg Nembutal i.v. after a tranquilizing dose of 11 mg/kg ketamine i.m.).

For three of the seven monkeys, AdSynEGFP was injected into temporal cortical areas (e.g., TEO and TEp), and for two of them, into area V4. The sixth animal received an injection in area V1 (Fig. 1). Cortical areas of interest were localized by direct visualization, subsequent to craniotomy and durotomy, in relation to sulcal landmarks (i.e. superior temporal and anterior or posterior middle temporal sulci or, for V4 and V1, the lunate sulcus). Two injections were made by a 10 µl Hamilton syringe, and a volume of 1.5 µl was injected at the depth of 1.5 mm (or 1.0 mm for area V1) below the pia. Injections were standardized to a volume of 1.5 µl of 1.0 x 10^{12} pfu/ml. After histological processing, the actual size of the injection site varied somewhat, but the core injection size was estimated as a cylinder, 1.0-1.5 mm in diameter. Injection sites were confined to the gray matter, and spanned through layers 1-6. For other purposes,

additional injections (not described here) were made of 10% biotinylated dextran amine (BDA; Molecular Probes, Eugene, OR; 1:1 mixture of 3,000 and 10,000 MW in 0.0125 M PBS) adjacent to the virus injection sites.

In one monkey, an injection was made in area V4 of cholera toxin subunit B conjugated with Alexa Fluor 488 (CTB-Alexa488; Invitrogen, Carlsbad, CA, USA). The tracer was diluted in 0.1M PB (to 1% concentration), and a volume of 1.5 µl was pressure injected, as described above. This monkey also had an injection of BDA in area V1, for other purposes.

Fixation and tissue preparation

After a post-injection survival of 18-22 days, the monkeys were re-anesthetized with ketamine and Nembutal (overdose, 75 mg/kg, i.p.), and perfused transcardially, in sequence, with saline for 2 minutes, 4 liters of 4% paraformaldehyde, and chilled 0.1 M phosphate buffer with 10%, 20%, and 30% sucrose (500 ml each). The brain was removed, and allowed to sink in 30% sucrose for cryoprotection. Two days later, the tissue was sectioned at 50 µm. Some sections were immediately scanned for EGFP fluorescence, but most of the tissue was reacted with antibody against EGFP, for immunofluorescence or further processing with 3,3' diaminobenzidine tetrahydrochloride (DAB)-immunohistochemistry. For the area V1 case, sequential sections were processed for DAB. For the other brains, we used a repeating series, where 5 sequential sections were processed for DAB, 10 by double fluorescence for anti-EGFP (or for BDA, processed by streptavidin conjugated with Alexa Fluor 594; as part of a separate confocal investigation), and 5 sections were available for

immunofluorescence for anti-EGFP and selected antibodies (as below).

Immunoperoxidase staining

Processing for AdSynEGFP injected materials was carried out by using affinity-purified rabbit anti-EGFP antibody (1:500) in 0.1 M PBS containing 0.5% Triton X-100 and 2% normal goat serum (PBS-TG), goat biotinylated anti-rabbit secondary antibody (Vector Laboratories, Burlingame, CA; 1:200 in PBS-TG), and ABC complex (ABC Elite kits; Vector Laboratories) at room temperature (one drop of reagent per 7 ml of 0.1 M PBS). Finally, EGFP was demonstrated by DAB histochemistry without nickel-ammonium sulfate. (This was in order to distinguish brown EGFP-positive cells from BDA-labeled fibers, which had been demonstrated in black, by DAB and nickel ammonium sulfate).

To visualize CTB-Alexa488, we used an immunoperoxidase reaction, with antibodies against Alexa Fluor 488. This provided some degree of enhancement, notably of dendritic filling, as well as a more permanent, DAB reaction product. After sectioning, free-floating sections were incubated for 1 hour in PBS-TG, then for 40-48 hours at 4 °C in PBS-TG containing anti-Alexa Fluor 488 antibody (1:1000, A-11094; lot No. 48619A; Invitrogen, Carlsbad, CA; immunogen; synthetic Alexa Fluor 488). Rabbit anti-Alexa Fluor 488 was characterized by immunoabsorption test using immunogen (see the data sheet of A-11094). Additionally, we determined there was no artifactual labeling, by comparing our histology sections with published connectivity studies. These sections were rinsed with PBS, and further incubated in PBS-TG containing goat biotinylated anti-rabbit secondary antibody (1:200; Vector Laboratories). After further rinses, processing was completed by DAB histochemistry with the addition of 0.03%

nickel ammonium sulfate.

Immunofluorescence staining

In the present study, we utilized the following antibodies: 1) Mouse anti-glutamic acid decarboxylase 67 (GAD67; MAB5406; lot No. 25080061; Chemicon, Temecula, CA; immunogen: recombinant GAD67). This reacts with the 67 kDa isoform of glutamate decarboxylase (GAD67) of rat, mouse, and human origins as shown by Western blotting (see the data sheet of MAB5406). 2) Rabbit anti-parvalbumin (PV; PV-28; lot No. 5.5; SWANT, Bellinzona, Switzerland; immunogen: rat muscle PV). This was characterized by immunoabsorption test, using recombinant rat PV (Xu et al., 2006). 3) Rat anti-somatostatin (SS; MAB354; lot No. 0602021758; Chemicon; immunogen: synthetic 1–14 cyclic SS conjugated to bovine thyroglobulin using carbodiimide). This was characterized by immunoabsorption tests, using synthetic SS peptide (Xu et al., 2006). 4) Rabbit anti-calretinin (CR; 7699/4; lot No. 18299; SWANT; immunogen: recombinant human CR). This was characterized by immunoabsorption test, using recombinant human CR (Xu et al., 2006). 5) Neuronal nitric oxide synthase (nNOS; AB1632; lot No. 23031420; Chemicon; immunogen: synthetic peptide corresponding to amino acids 724-739 of human brain NOS). This was characterized by immunoabsorption test, using immunogen peptide (see the data sheet of AB1632). 6) Rabbit anti-muscarinic acetylcholine receptor m2 (AB5166; lot No. 21071386; Chemicon; immunogen; recombinant human m2 corresponding to amino acids 225-356). This reacts with the 65 kDa isoform as shown by Western blotting blotting (see the data sheet of AB5166). 7) Rabbit or guinea pig anti-EGFP (immunogen; recombinant EGFP), were characterized by immunoabsorption test using immunogen. Additionally, we

determined there was no artifactual labeling, by comparing our histology sections with published connectivity studies.

For the six monkeys, sections were incubated for 40-48 hours in the cold room in a mixture of two or three different antibodies. In order to visualize neurons retrogradely labeled by AdSynEGFP, every section was incubated with the affinity-purified guinea pig anti-EGFP antibody (1:500). The additional antibodies were chosen from the following: anti-GAD67 monoclonal mouse antibody (1:400), anti- PV polyclonal rabbit antibody (1:400), anti-SS monoclonal rat antibody (1:400), anti- CR polyclonal rabbit antibody (1:1000), anti-nNOS polyclonal rabbit antibody (1:400), and anti-m2 muscarinic receptor polyclonal rabbit antibody (1:400). Finally, the sections were incubated for 1.5 hours in PBS-TG containing the suitable combination of secondary antibodies. These were chosen from the following: Alexa Fluor 488-conjugated anti-guinea pig IgG polyclonal goat antibody (Molecular Probes; 1:200), Alexa Fluor 594-conjugated anti-rat IgG polyclonal goat antibody (Molecular Probes; 1:200), Alexa Fluor 350-conjugated anti-mouse IgG polyclonal goat antibody (Molecular Probes; 1:200), and Alexa Fluor 350-conjugated anti-rabbit IgG polyclonal goat antibody (Molecular Probes; 1:200). Sections were mounted on glass slides and coverslipped with IMMU-MOUNT (Thermo Shandon, Pittsburgh, PA). See Table 1 for further description of antibodies.

Control for specificity of AdSynEGFP label

As a technical control, one adult rat received a pressure injection in area V1 of AdSynEGFP (0.3 µl of 1.0 x 10^{12} pfu/ml) mixed with cholera toxin subunit B

conjugated Alexa Fluor 594 (CTB-Alexa594; Invitrogen; 0.2% concentration). After a survival time of 8 days, the rat was reanesthetized with chloral hydrate (350 mg/kg body weight), and perfused transcardially with 100 ml of saline, followed by 300 ml of 4% paraformaldehyde in 0.1 M phosphate buffer, pH 7.4. After cryoprotection with 30% sucrose in PBS, the brain was cut at 60-µm-thick frontal sections on a freezing microtome. Neurons retrogradely labeled by EGFP and/ or CTB-Alexa594 could be observed (antibody enhancement was not used in this tissue). Transport was assessed by inspecting regions known to project to the injected site; namely, ipsi- and contralateral cortex, thalamus and claustrum. In all these regions, double-labeled neurons were found. In particular, neurons in the white matter (putative GABAergic neurons) were observed. EGFP-expressing neurons were positive for CTB-Alexa594. Some neurons labeled with CTB-Alexa594 were not co-labeled with EGFP, but this is expected because 1) the concentration of CTB-Alexa594 is higher than that of AdSynEGFP, 2) there may be the different transport efficacy. We found no evidence of unusual labeling by EGFP, which might have been an indication of artifactual label. (see the supplementary figure).

Data analysis

Sections were scanned using a 10x or 20x objective, to identify putative non-pyramidal neurons. Morphometric analyses were carried out on DAB-reacted material. Soma size was assessed by generating digital images (using a 40x objective) and tracing the soma outlines on the computer screen, using the computer mouse. To assure precise measurements, we selected soma which were completely within the 50 µm-thick section, and measured the maximum size at a suitable focus depth. Pixels in the selected area

(i.e., individual somata) were analyzed by AxioVision 3.1 software (Carl Zeiss, Jena, Germany) and calculated as square microns. The maximum length of dendrite was ascertained by tracing in Image J software (National Institutes of Health, USA). All photographs were taken as digital images (Axioskop 2 plus microscope, Carl Zeiss). The images were merged and adjusted for contrast and/or brightness to match the real image, by using image software (Adobe Photoshop 7.0, Adobe, San Jose, CA).

Immunofluorescence was observed under an epifluorescence microscope, with appropriate filter sets for Alexa Fluor 350 (peak excitation, 346 nm; peak emission, 442 nm), Alexa Fluor 488 (peak excitation, 495 nm; peak emission, 519 nm) and 594 (peak excitation, 590 nm; peak emission, 617 nm). Since all EGFP-expressing neurons were evident in this material (pyramidal as well as non-pyramidal), sections could be used to control that GABAergic chemical markers were not found in EGFP-labeled pyramidal neurons, but only in EGFP-labeled non-pyramidal neurons.

Cortical areas were identified by comparison with schemata, in relationship to AP levels and sulcal patterns, in previously published papers (e.g. Van Essen et al., 1986; Distler et al., 1993; Lewis and Van Essen, 2000) and a recently published (Saleem and Logothetis, 2007). For areas V2 and V3, these landmarks are sufficient for clear identification. Identifications of other, more rostral areas should be regarded as provisional, due to the variability of individual brains.

Results

Injection of CTB-Alexa488 in area V4

Retrograde transport of this vector, AdSynEGFP from an injection site and subsequent infection of projecting neurons is a new technique (Tomioka and Rockland, 2006). To control for possible artifactual label, we injected CTB-Alexa488 in area V4 in one animal (Fig. 1). This has been a common tracer, and its transport specificity is generally accepted (e.g., Angelucci and Sainsbury, 2006). This injection resulted in obvious label of putative non-pyramidal neurons in the white matter (Fig. 2). These were comparatively numerous (>30 neurons per section) at the same anterior-posterior levels as the injection site, where they occurred in the white matter 0.5-3.0 mm below the injection site, as well as up to 1.5cm medially. Neurons tended to be separated by 200-250µm (range: 100-300 µm). Labeled neurons continued in the white matter for about 0.5 mm anterior and posterior to the injection, but were markedly fewer (2-3 per section), and were confined to 2-3 mm below layer 6. Possible non-pyramidal neurons in the gray matter could not be ascertained, as morphological criteria were insufficient for identification, and we did not carry out immuno-processing in this brain. (Also, see **Methods***: Control for specificity*)

Global distribution of EGFP-labeled neurons

Pressure injections of AdSynEGFP in areas V1, V4, TEO, or TEp consistently resulted in strong EGFP expression in pyramidal neurons projecting to the injection site (Fig. 1). After immunoreaction, Golgi-like filling of dendritic spines was routinely achieved. Some axon collateral filling was evident, but principally, this vector is effective for retrograde filling. Most of the EGFP-expressing neurons could easily be identified as

pyramidal because of the morphology of the somata and dendritic arbor, and the existence of numerous dendritic spines. Their distribution was consistent with that of previous reports using injections of traditional retrograde tracers in these areas (e.g., Van Essen et al., 1986; Distler et al., 1993). However, in addition, some of the EGFP-expressing neurons were identifiable as non-pyramidal (Fig. 3) because of their aspiny or sparsely spinous dendrites (Peters and Jones, 1984).

Some non-pyramidal neurons could be discerned in the immediate vicinity of the injections. These are assumed to correspond to classical GABAergic interneurons. More particularly, however, in each of the six cases, GABAergic-like neurons were evident up to 1.5 cm distant from the injection site, both in gray and white matter, but mainly in the white matter (Figs. 4, 5).

In two brains that were intensively analysed, we scored 110 neurons in the white matter and 25 in the gray matter (R116, injection in posterior area TE), or 107 neurons in the white matter and 21 in the gray matter (case 313, injection in TEp). In a third brain (R109), with an injection in area V4, 52 neurons were scored in the white matter and 5 in the gray matter. Two other brains with an injection in area TEp (case 135) or V4 (case 131) were used for confirmation only; and case 146 (injection in area V1) also was not quantified. In the white matter, neurons occurred in both the subgriseal and deeper compartments, but mainly in the deeper (beyond 0.5 mm below layer 6). In case R116 (TEO injection), non-pyramidal neurons were comparatively frequent in the lower bank of the superior temporal sulcus, in the location of FST, PIT, or TEm/TEa (Distler et al., 1993; Cusick et al., 1995; Lewis and Van Essen, 2000). After the V4 injection,

white matter neurons occurred up to 7.0 mm medial to the injection, and 2.0-3.0 mm both anterior and posterior. In the gray matter, neurons were again in the lower bank and depth of the superior temporal sulcus (at a level corresponding to section 4 in Fig. 2 of Distler et al., 1993).

After the injection in area V1, non-pyramidal neurons were evident in the posterior bank of the lunate sulcus (LS; area V2), in the depth of the LS (area V3) and in the annectant gyrus (area V3). These were in layer 3, with an occasional neuron in layer 2 or 1 (Figs. 3, 5). They occurred at the rate of one or two per section in these areas (Fig. 5). Abundant pyramidal neurons occurred in these areas, as well as in area V4 and MT, but non-pyramidal neurons were not detected in V4 or MT or anteriorly. In the white matter, numerous neurons (>20 per section) occurred near the injection, between the lateral operculum (V1) and the underlying posterior bank of the LS (Fig. 5D); and smaller numbers continued in this region of the white matter for 2.0-3.0 mm both anterior and posterior to the injection.

The morphology of long-distance projecting GABAergic-like neurons

Non-pyramidal neurons in the gray matter (Fig. 3) had relatively large soma (Table 2: 196.8 ± 56.5 μm^2, n = 42). They occurred, in association with labeled pyramidal neurons, mainly in layer 3. After the injection in V1, non-pyramidal neurons in V2 and V3 were only in the supragranular layers. After the V4 and temporal injections, some neurons could be found in the deeper layers; but only one clear example was identified in layer 1. Most of these neurons resembled multipolar or bitufted cells, on the basis of dendritic configuration. Several relatively long dendrites could be seen emanating from

the soma; and in partial serial sections, a single dendrite could be followed for 235-580 µm. For most of these neurons, the dendrites were not entirely smooth, but were sparsely covered with spines (Fig. 3B). Varying lengths of proximal axon could often be discerned, but usually this was very limited. When detectable, the axon was only sparsely studded with terminal specializations. These were a mix of beaded and stalked boutons (Fig. 6B).

In the white matter, the GABAergic-like population is characterized by a small soma (Table 2: 159.2 ± 40.1 μm^2, n = 179). The average soma size of the gray matter neurons vs. white matter neurons was significantly different ($p < 0.001$ with student t-test). Typically, there were two to four dendrites projecting from the soma. These could be radiate or, commonly, extended horizontally from the soma (for 120-550 µm), parallel to the overlying layer 6 (Fig. 7). Like the non-pyramidal neurons in the gray matter, these were usually not clustered, but 2-3 neurons could occur in one section. In one brain (case 135) with a particularly distinct fiber bundle, 5-7 neurons (per section) could be seen in the white matter over a distance of about 4.0 mm dorso-ventral and 1.5 mm anterior-posterior. In the white matter, axons could often be seen in their proximal, perisomatic segments, but could not be followed over longer distances. (Axons were thinner than dendrites and less wavy. In addition, the terminal specializations – mixed beads and stalks – were distinctive from even sparsely spinous dendrites.)

Neurochemical markers of long-distance projecting GABAergic neurons

To confirm the morphological identification of these non-pyramidal neurons, we first ascertained that EGFP-expressing non-pyramidal neurons (n=139) were positive for

GAD67. Next, we further screened for parvalbumin (PV), somatostatin (SS), and calretinin (CR). Triple labeling (in addition to anti-EGFP and anti-GAD67) demonstrated (Fig. 8 and Table 3) that most of these neurons (90%: 74/82) exhibited SS immunoreactivity, many (14%: 5/36) exhibited CR immunoreactivity, and none (0/21) exhibited PV immunoreactivity. The SS-, GAD67- and EGFP-triple positive neurons occurred mainly in the white matter but also in layers 3, 5 and 6. Finally, we carried out triple labeling for EGFP and SS, with CR, nNOS, or m2 muscarinic receptor. From this, we found that almost all SS-positive long-distance projecting GABAergic neurons exhibited nNOS (16/17) and m2 (20/21) immunoreactivity.

Discussion

We report that GABAergic neurons in the white matter and a smaller number in the gray matter project to cortical areas in the macaque. Projecting neurons were detected after injections of AdSynEGFP in areas V1, V4, and several subdivisions of temporal association cortex (TEO, TEp). After the injection in area V1, scattered non-pyramidal neurons were found in areas V2 and V3, intermingled in a field of pyramidal neurons, but were not found in V4 or MT. In all the other cases, a few labeled neurons were consistently found in the lower lip (area TEm) and lower bank of the STS (area FST or PIT), with a very few neurons scattered in temporal cortex anterior to the injection. For all the six brains, EGFP-expressing neurons were more numerous in the white matter, occurring at distances up to 1.5 cm medially or anteriorly from the injection.

"Long-distance" is meant as a neutral term, principally to denote that these gray matter

GABAergic neurons are not "intrinsic," where "intrinsic" is taken to mean within 500 µm of an injection site. After the injection in area V1, neurons were clearly long-distance and inter-areal; but the "intra-areal" vs. "inter-areal" distinction was less obvious for some of the scoring after temporal injections, as well as for white matter neurons near the injection site. More discussion about nomenclature is desirable, but may require additional information about subtypes and functional significance."

Technical Considerations

In these experiments, the Golgi-like morphological detail produced by the AdSynEGFP vector significantly aided our detection of non-pyramidal projecting neurons, especially in the gray matter, where they were intermingled with and obscured by more numerous pyramidal neurons. It was then important to process selected, non-DAB reacted sections for immunofluorescence (anti-EGFP with anti-GAD and/or other antibodies).

As the AdSynEGFP vector is a new tracer, a natural concern is whether the apparent labeling could be nonspecific. We think this is unlikely for several reasons. First, labeled neurons were evident in the white matter after injections in area V4 of the conventional tracer CTB-Alexa488. Second, co-injection of AdSynEGFP and CTB-Alexa594 in rat area V1 demonstrated neurons double-labeled for both tracers in the expected structures (ipsi- and contralateral cortex, thalamus, and claustrum, as well as white matter; see **Methods** for further description, and supplementary figure). Third, our results are consistent with previous reports (see below), which described retrogradely labeled neurons in the white matter, and GABAergic projection neurons in the gray matter.

Previous studies

Neurons in the white matter have been extensively investigated, by histochemistry (Sandell, 1986; Egberongbe et al., 1994; Yan et al., 1996; Smiley et al., 2000; Garbossa et al., 2005; Colombo and Bentham, 2006) and, to a lesser extent, by intracellular fills (Clancy et al., 2001). There have been consistent reports over the years that these neurons are labeled by retrograde tracer injections. Labeled neurons were reported in the white matter below area 18 in the ferret, after HRP injections in area 17 (Rockland, 1985), in the white matter below several frontal areas in macaque after WGA-HRP injections in the medio-dorsal thalamus (Fig. 12 in Giguere and Goldman-Rakic, 1988; and personal observations), in the white matter of rats after fluorescent tracer injections in the neocortex (Clancy and Cauller, 1999; Clancy et al., 2001), and in the white matter of cats after WGA-HRP injections in several sensory areas (Higo et al., 2007).

GABAergic projecting neurons in the gray matter have been identified in several studies, using a variety of double-labeling techniques (see **Introduction**). Although most investigations have been of cortically projecting long distance GABAergic neurons, Jinno and Kosaka (2004) reported that some corticostriatal neurons are GABAergic in mice. Fluorogold (FG) injections in the caudal striatum resulted in a small number of neurons (3-5% of all FG-labeled neurons, sampled in the somatosensory and retrosplenial cortices), co-labeled for FG and GAD, or for FG, GAD, and parvalbumin. This result was confirmed by ultrastructural identification of GAD (+) cortiocostriatal terminals (labeled by injection of the anterograde tracer PHA-L).

In the gray matter, the number of GABAergic projecting neurons has been variably estimated as 10% of the GABAergic population (Peters et al., 1990) or less than 1% (McDonald and Burkhalter, 1993; Molnar and Cheung, 2006). This may well be species and region dependent. Regional variation has been noted in the distribution of white matter interstitial neurons, as labeled by NADPH diaphorase (Garbossa et al., 2005; Cruz-Rizzolo et al., 2006); and area-specific differences have also been noted in the percentage of corticocortical terminals double-labeled for PHA-L and GABA in guinea pigs after injections in perirhinal areas 35 and 36 (Pinto et al., 2006).

Circuitry and functional significance

Several studies have demonstrated specific inputs to white matter neurons. Cortical injections of PHA-L in kittens and cats revealed synapses onto dendritic shafts and spines of white matter neurons (Shering and Lowenstein, 1994). Whole cell recording from white matter neurons ("subplate neurons" at early stages in development) in slices of somatosensory cortex of young rats have described functional synaptic inputs from the thalamus, from deep layers of the cortical plate, and from other neurons in the subplate (Hanganu et al., 2002). In GAD67-GFP knock-in mice (Tomioka et al., 2005), confocal and electron microscopy revealed that the dendrites of neurons double-labeled for GFP and fast blue (transported from injections in the motor cortex) had synapses positive for VGluT1 but not VGluT2 (transporters indicative, respectively, of cortical and thalamic terminations (Fujiyama et al., 2001)). The apparent discrepancy about thalamic input between these two studies may be due to different ages, species, and/or areas. Finally, white matter GABAergic neurons, which express m2 muscarinic receptors, are likely to receive a cholinergic innervation, presumably from nucleus

basalis of Meynert (Smiley et al., 1998). A recent study of GABAergic neurons projecting from perirhinal to entorhinal cortex in guinea pig, demonstrates that these neurons are presynaptically inhibited by m2 receptor activation (Apergis-Schoute et al., 2007).

Intracellular fills with biocytin in rat visual cortex have demonstrated dense terminations from white matter neurons to overlying cortex (Clancy et al., 2001); and serial reconstructions of GFP-expressing white matter neurons in mice have similarly demonstrated projecting axons (Tomioka et al., 2005). So far, only sparse data are available on the important question of the postsynaptic targets of these neurons. In one instance, after gray matter injections in the guinea pig, terminations double-labeled for GABA and PHA-L were found to terminate predominantly on GABA-negative dendrites, suggestive of a specific GABAergic network (Pinto et al., 2006). Another unanswered question is whether these neurons may have widespread axon collateral branches. In this case, they could be well-positioned to influence wide-sector effects, possibly including action across neuronal networks (Cossart et al., 2005; Buzsaki, 2006).

In early development, subplate neurons in the white matter play a key role in the establishment of thalamocortical circuitry, and are necessary for the formation of orientation maps and the sharpening of orientation tuning in cat visual cortex (Allendoerfer and Shatz, 1994; Arber, 2004; Kanold and Shatz, 2006). A transient population of neurons in the corpus callosum of cats has been proposed to play a role in axon guidance (Riederer et al., 2004). The role of long-distance projecting GABAergic

neurons in the adult, either in the white or gray matter is not known. One clue regarding their functional significance may be the finding that a high percentage of long-distance projecting GABAergic neurons are positive for nNOS. Nitric oxide has been proposed as a diffusible factor implicated in the regulation of vasodilation, neural plasticity, and learning (Bredt and Snyder, 1992; Bon and Garthwaite, 2003).

Another clue is the neurochemical heterogeneity of these neurons. While the majority of these neurons are positive for SS, this group can be further subdivided on the basis of co-localization with CR. That is, we found that about 23% of the sample was SS (+) and CR (+), but 77% were SS (+) and CR (-). None of the neurons were triple-labeled for PV. From this, a reasonable prediction is that further work will reveal some degree of functional heterogeneity as well.

Acknowledgements

We thank Ms. Hiromi Mashiko, Mr. Adrian Knight, and Mr. Daniel Potapov for their excellent technical assistance, Ms. Yoshiko Abe for assistance in quantification, and Dr. Toshio Miyashita and Ms. Michiko Fujisawa for help with manuscript preparation.

LITERATURE CITED

Allendoerfer KL, Shatz CJ. 1994. The subplate, a transient neocortical structure: its role in the development of connections between thalamus and cortex. Annu Rev Neurosci 17:185-218.

Angelucci A, Sainsbury K. 2006. Contribution of feedforward thalamic afferents and corticogeniculate feedback to the spatial summation area of macaque V1 and LGN. J Comp Neurol 498: 330-351.

Apergis-Schoute J, Pinto A, Pare D. 2007. Muscarinic control of long-range GABAergic inhibition within the rhinal cortices. J Neurosci 27:4061-4071.

Arber S. 2004. Subplate neurons: bridging the gap to function in the cortex. Trends Neurosci 27: 111-113.

Bon CL, Garthwaite J. 2003. On the role of nitric oxide in hippocampal long-term potentiation. J Neurosci 23:1941-1948.

Bonin G von, Bailey P. 1947. The neocortex of Macaca mulatta. Urbana, IL: University of Illinois Press.

Bredt DS, Snyder SH. 1992. Nitric oxide, a novel neuronal messenger. Neuron 8:3-11.

Buzsaki G. 2006. Rhythms of the Brain. Oxford: Oxford University Press.

Clancy B, Cauller LJ. 1999. Widespread projections from subgriseal neurons (layer VII) to layer I in adult rat cortex. J Comp Neurol 407:275-286.

Clancy B, Silva-Filho M, Friedlander MJ. 2001. Structure and projections of white matter neurons in the postnatal rat visual cortex. J Comp Neurol 434:233-252.

Colombo JA, Bentham C. 2006. Immunohistochemical analysis of subcortical white matter astroglia of infant and adult primate brains, with a note on resident neurons. Brain Res 1100:93-103.

Cossart R, Bernard C, Ben-Ari Y. 2005. Multiple facets of GABAergic neurons and synapses: multiple fates of GABA signalling in epilepsies. Trends Neurosci 28:108-115.

Cruz-Rizzolo R, Horta-Junior JA, Bitterncourt JC, Ervolino E, de Oliveira JA, Casatti CA. 2006. Distribution of NADPH-diaphorase-positive neurons in the prefrontal cortex of the Cebus monkey. Brain Res 1083:118-133.

Cusick CG, Seltzer B, Cola M, Griggs E. 1995. Chemoarchitectonics and corticocortical terminations within the superior temporal sulcus of the rhesus monkey: evidence for subdivisions of superior temporal polysensory cortex. J Comp Neurol. 360:513-535.

DeFelipe J. 1997. Types of neurons, synaptic connections and chemical characteristics of cells immunoreactive for calbindin-D28K, parvalbumin and calretinin in the neocortex. J Chem Neuroanat 14:1-19.

DeFelipe J, Farinas I. 1992. The pyramidal neuron of the cerebral cortex: morphological and chemical characteristics of the synaptic inputs. Prog Neurobiol 39:563-607.

Distler C, Boussaoud D, Desimone R, Ungerleider LG. 1993. Cortical connections of inferior temporal area TEO in macaque monkeys. J Comp Neurol 334:125-150.

Egberongbe YI, Gentleman SM, Falkai P, Bogerts B, Polak JM, Roberts GW. 1994. The distribution of nitric oxide synthase immunoreactivity in the human brain. Neuroscience 59:561-578.

Fabri M, Manzoni T. 1996. Glutamate decarboxylase immunoreactivity in corticocortical projecting neurons of rat somatic sensory cortex. Neuroscience 72:435–448.

Fabri M, Manzoni T. 2004. Glutamic acid decarboxylase immunoreactivity in callosal projecting neurons of cat and rat somatic sensory areas. Neuroscience 123:557–566.

Fujiyama F, Furuta T, Kaneko T. 2001. Immunocytochemical localization of candidates for vesicular glutamate transporters in the rat cerebral cortex. J Comp Neurol 435:379-387.

Garbossa D, Fontanella M, Tomasi S, Ducati A, Vercelli A. 2005. Differential distribution of NADPH-diaphorase histochemistry in human cerebral cortex. Brain Res 1034:1-10.

Giguere M, Goldman-Rakic PS. 1988. Mediodorsal nucleus: areal, laminar, and tangential distribution of afferents and efferents in the frontal lobe of rhesus monkeys. J Comp Neurol 277:195-213.

Gonchar YA, Johnson PB, Weinberg RJ. 1995. GABA-immunopositive neurons in rat neocortex with contralateral projections to S-I. Brain Res 697:27-34.

Gonzalez-Albo MC, Elston GN, DeFelipe J. 2001. The human temporal cortex: characterization of neurons expressing nitric oxide synthase, neuropeptides and calcium-binding proteins, and their glutamate receptor subunit profiles. Cereb Cortex 11:1170-1181.

Hanganu IL, Kilb W, Luhmann HJ. 2002. Functional synaptic projections onto subplate neurons in neonatal rat somatosensory cortex. J Neurosci 22:7165-7176.

Higo S, Udaka N, Tamamaki N. 2007. Long-range GABAergic projection neurons in the cat neocortex. J Comp Neurol 503: 421-431.

Jinno S, Kosaka T. 2004. Parvalbumin is expressed in glutamatergic and GABAergic corticostriatal pathway in mice. J Comp Neurol 477:188-201.

Kanold PO, Shatz CJ. 2006. Subplate neurons regulate maturation of cortical inhibition and outcome of ocular dominance plasticity. Neuron 51:627-638.

Kostovic I, Rakic P. 1980. Cytology and time of origin of interstitial neurons in the white matter in infant and adult human and monkey telencephalon. J Neurocytol 9:219-242.

Kostovic I, Rakic P. 1990. Developmental history of the transient subplate zone in the visual and somatosensory cortex of the macaque monkey and human brain. J Comp Neurol 297:441-470.

Lewis JW, Van Essen DC. 2000. Mapping of architectonic subdivisions in the macaque monkey, with emphasis on parieto-occipital cortex. J Comp Neurol 428:79-111.

McDonald CT, Burkhalter A. 1993. Organization of long-range inhibitory connections with rat visual cortex. J Neurosci 13:768–781.

Molnar Z, Cheung AFP. 2006. Towards the classification of subpopulations of layer V pyramidal projection neurons. Neurosci Res 55: 105-115.

Peters and Jones. 1984. Cerebral Cortex Volume 1. Cellular Components of the Cerebral Cortex. Plenum Press. 107-121.

Peters A, Payne BR, Josephson K. 1990. Transcallosal non-pyramidal cell projections from visual cortex in the cat. J Comp Neurol 302:124-142.

Pinto A, Fuentes C, Pare D. 2006. Feedforward inhibition regulates perirhinal transmission of neocortical inputs to the entorhinal cortex: ultrastructural study in guinea pigs. J Comp Neurol 495:722-734.

Riederer BM, Berbel P, Innocenti GM. 2004. Neurons in the corpus callosum of the cat during postnatal development. Eur J Neurosci 19:2039-2046.

Rockland KS. 1985. Anatomical organization of primary visual cortex (Area 17) in the ferret. J Comp Neurol 241:225-236.

Saleem KS, Logothetis NK. 2007. A combined MRI and histology atlas of the rhesus monkey brain. Elsevier.

Sandell JH. 1986. NADPH diaphorase histochemistry in the macaque striate cortex. J Comp Neurol 251:388-397.

Shering AF, Lowenstein PR. 1994. Neocortex provides direct synaptic input to interstitial neurons of the intermediate zone of kittens and white matter of cats: a light and electron microscopic study. J Comp Neurol 347:433-443.

Smiley JF, Levey AI, Mesulam MM. 1998. Infracortical interstitial cells concurrently expressing m2-muscarinic receptors, acetylcholinesterase and nicotinamide adenine dinucleotide phosphate-diaphorase in the human and monkey cerebral cortex. Neuroscience 84:755-769.

Smiley JF, McGinnis JP, Javitt DC. 2000. Nitric oxide synthase interneurons in the monkey cerebral cortex are subsets of the somatostatin, neuropeptide Y, and calbindin cells. Brain Res 863:205-212.

Tomioka R, Rockland KS. 2006. Improved Golgi-like visualization in retrogradely projecting neurons after EGFP-adenovirus infection in adult rat and monkey. J Histochem Cytochem 54:539-548.

Tomioka R, Okamoto K, Furuta T, Fujiyama F, Iwasato T, Yanagawa Y, Obata K, Kaneko T, Tamamaki N. 2005. Demonstration of long-range GABAergic connections distributed throughout the mouse neocortex. Eur J Neurosci 21:1587–1600.

Van Essen DC, Newsome WT, Maunsell JH, Bixby JL. 1986. The projections from striate cortex (V1) to areas V2 and V3 in the macaque monkey: asymmetries, areal boundaries, and patchy connections. J Comp Neurol 244:451-480.

Xu X, Roby KD, Callaway EM. 2006. Mouse cortical inhibitory neuron type that coexpresses somatostatin and calretinin. J Comp Neurol 499:144-160.

Yan XX, Jen LS, Garey IJ. 1996. NADPH-diaphorase-positive neurons in primate cerebral cortex colocalize with GABA and calcium-binding proteins. Cereb Cortex 6:524-529.

Figure 1

(A) Schematic brain diagram to show the location of six AdSynEGFP injection sites (cortical territories are from the map of von Bonin and Bailey, 1947). Injections were placed at the border of anterior and posterior TE (white and dotted circles), in TEO (asterisk), in V4 (black and white diamonds), and in area V1 (black circle). The injection of cholera toxin subunit B in a seventh monkey is similar in location to the black diamond. The thick vertical line ("B") corresponds to the level of the coronal section shown in (B). Numbered thinner lines (138, 91, 62, 49) indicate the approximate anterior-posterior levels of the sections shown in Fig. 4. (B) EGFP expression (visualized by immuno-peroxidase processing) after adenovirus injection in TEO. Abundant EGFP-expressing pyramidal neurons were observed in the superior temporal sulcus and other cortical areas, consistent with previous reports using other retrograde tracers. The region within the rectangle is re-photographed at higher magnification in (C). Darkened area (arrow) corresponds to the fringe of the injection site. (C) EGFP-expressing neurons in layers 3 and 5 in the lower bank of the superior temporal sulcus. Scale bars = 1.0 cm in B, 0.5 mm in C.

Figure 2

Photomicrographs showing retrogradely labeled neurons in the white matter (putative non-pyramidal neurons) after an injection of CTB-Alexa488 in area V4. (A) A portion of the injection site (at left) and scattered neurons in the subjacent white matter. This field is higher magnification of the boxed "A" region, from the histological section inset in (C). (B) Scattered neurons are labeled in the medial white matter. This field is higher magnification of the boxed "B" region from the histological section (inset in (C). Short

fragments of BDA-labeled fibers (labeled by an injection of BDA in area V1, as part of another study) are evident further medially, at right. (C) Higher magnification of labeled neurons below the injection site (from the boxed "C" region in (A)). Inset is low magnification of a coronal histology section, showing the anterior edge of the injection site and the location of the two fields shown with labeled cells. (D) Higher magnification of labeled neurons from the medial location, at the "D" box in (B). Scale bars= 500 µm in B (for A and B), 50 µm in D (for C and D), 5 mm in the inset.

Figure 3

Photomicrographs showing retrogradely labeled non-pyramidal neurons in the gray matter after injections of AdSynEGFP. (A) Neuron in layer 3 (arrow) of the depth of the superior temporal sulcus (STS; section 91 in Fig. 4) after an injection in area TEO (case R116). Two adjacent pyramidal neurons are evident (arrowheads). (B) Another neuron in layer 3 (arrow) of the lower bank of the STS (section 62 in Fig. 4), in case R116. Dendrites are sparsely spinous (see arrows in higher magnification inset, which is from the region at arrowhead in (B)). (C) Neuron in layer 3 of the lower bank of the STS, in case 135 (injection in posterior TE). (D) Neuron at the border of layers 1 and 2 in area V2, after the injection in V1 (Fig. 5). Scale bars = 100 µm in A-D, 5 µm in the inset (C same as in B).

Figure 4

(A-D) Coronal section outlines from four AP levels in case R116 (injection of AdSynEGFP in area TEO), where medial is at the right. Numbers indicate AP progression, where smaller numbers are more posterior. Dots represent

EGFP-expressing neurons, pyramidal (small dots) and non-pyramidal (large dots), where one dot = one neuron. Shaded regions = lateral ventricle. Scale bar = 1.0 cm.

Figure 5

(A-C) Three coronal section outlines illustrating the distribution of non-pyramidal neurons in the gray matter, in areas V2 and V3 after the injection in area V1. Smaller numbers are more posterior, large dots = non-pyramidal neurons and small dots = pyramidal neurons. For simplicity, only non-pyramidal neurons are shown in V2 and V3. Short lines denote V1/V2 borders on the lateral surface. The peri-injection zone is at section 105. (D) A higher magnification view at right shows the distribution of white matter neurons in the immediate vicinity of the injection (shaded portion; section 107). There was no invasion of the white matter, either by injection needle or halo. Scale bar = 5 mm in A-C, 1 mm in D.

Figure 6

Axonal boutons are sparsely distributed in the proximal portion. (A) Non-pyramidal neuron in layer 3 of area V3 (section 105, Fig. 5). Arrow indicates axon. (B) Higher magnification from the arrow in (A). Terminal specializations are both beaded (upper arrow) and stalked (bottom two arrows). Scale bars = 200 μm in A, 40 μm in B.

Figure 7

Photomicrographs showing retrogradely labeled non-pyramidal neurons in the white matter after injections of AdSynEGFP. (A- E) Retrogradely labeled neurons at two AP levels from case 313 (injection in area TEp; A and D are from below the STS, about 3.0

mm apart). White matter neurons, as shown here, tend to have a narrow, compressed dendritic field, in contrast with the larger dendritic field of neurons in the gray matter (compare Fig. 2). Rectangles in (A) and (D) are re-photographed at higher magnification in (B), (C), and (E). (F) Several neurons are evident in the white matter, situated in a bundle of labeled axons issuing from the vicinity of the injection site (case 135). (G, H) Higher magnification from the rectangles in (F). Scale bars = 500 µm in A, D; 100 µm in B, C, E; 1.0 mm in F; 200 µm in G, H.

Figure 8

Fluorescent photomicrographs showing neurochemical characterization of EGFP-labeled non-pyramidal neurons. (A) EGFP-expressing non-pyramidal neuron (arrow) in the white matter (injection of AdSynEGFP in TEO, case R116). This is co-labeled with somatostatin (A') and GAD67 (A"). (B) EGFP-expressing non-pyramidal neuron (arrow) in layer 3 (from section 91, Fig. 4). This is co-labeled with somatostatin (B') and nNOS (B"). (C) EGFP-expressing non-pyramidal neuron (arrow) in the white matter, is positive for somatostatin (C') and calretinin (C"). (D) EGFP-expressing neuron (arrow) in the white matter, positive for somatostatin (D') and m2 muscarinic receptor (D"). Scale bars = 50 µm.

Supplementary figure

Photomicrographs showing retrogradely labeled neurons after injections of AdSynEGFP mixed with CTB-Alexa594 in the rat primary visual area. (A) Retrogradely EGFP-labeled neuron (putative non-pyramidal neuron) in the white matter (arrow). (B-B") Area around arrow in (A) was re-photographed at higher magnification. The

EGFP-labeled neuron is positive for CTB-Alexa594 (arrows). (C-C") Some EGFP-labeled neurons are positive for CTB-Alexa594 in the ipsilateral neocortex (arrows). (D-D") Some EGFP-labeled neurons are positive for CTB-Alexa594 in the ipsilateral thalamus (arrows). (E-E") core injection size was estimated as a cylinder, 0.5 mm in diameter. Injection sites were confined to the gray matter. Scale bars = 200 µm in A and E, 50 µm in B-D.

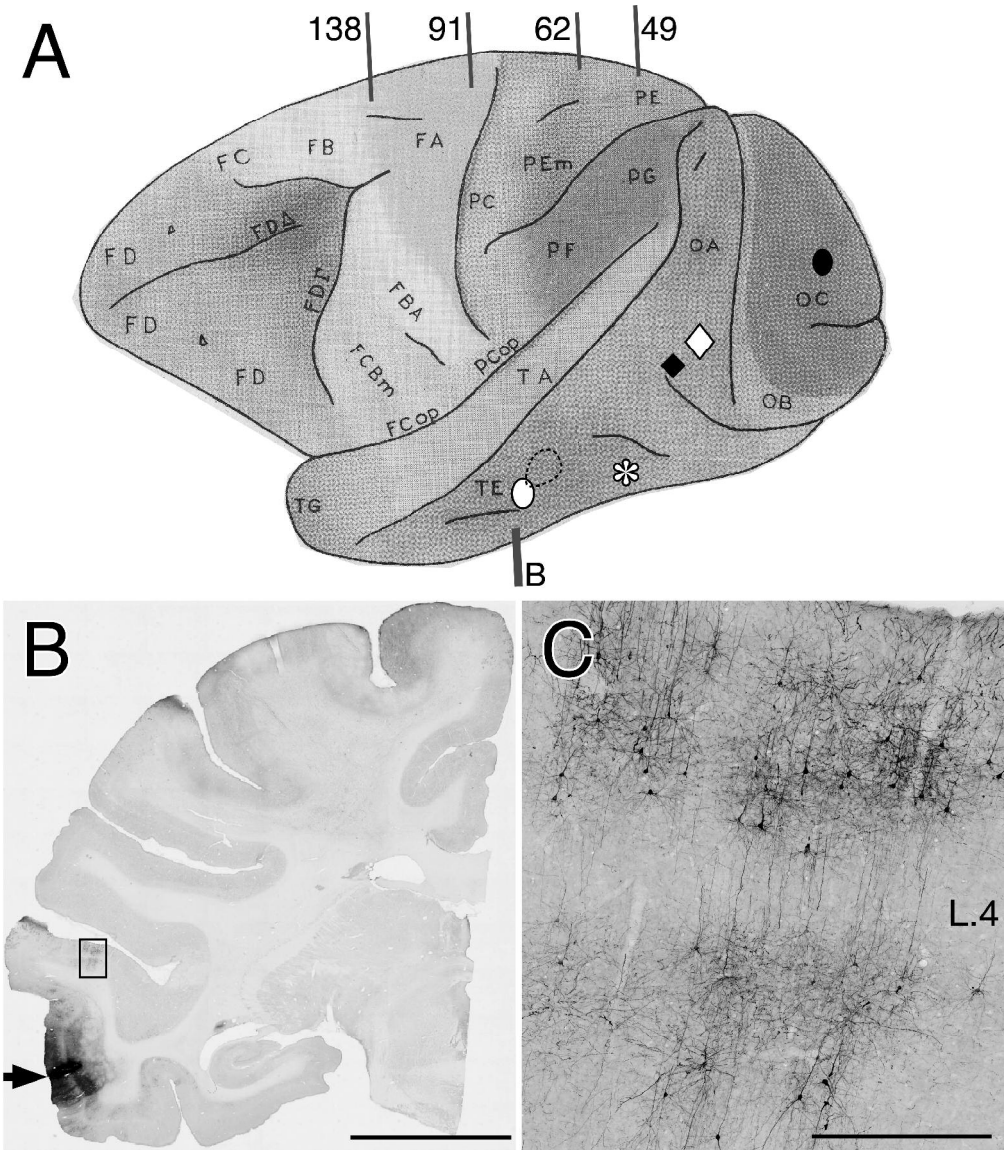

Figure 1 (A) Schematic brain diagram to show the location of six AdSynEGFP injection sites (cortical territories are from the map of von Bonin and Bailey, 1947). Injections were placed at the border of anterior and posterior TE (white and dotted circles), in TEO (asterisk), in V4 (black and white diamonds), and in area V1 (black circle). The injection of cholera toxin subunit B in a seventh monkey is similar in location to the black diamond. The thick vertical line (□❝B□❞) corresponds to the level of the coronal section shown in (B). Numbered thinner lines (138, 91, 62, 49) indicate the approximate anterior-posterior levels of the sections shown in Fig. 4. (B) EGFP expression (visualized by immuno-peroxidase processing) after adenovirus injection in TEO. Abundant EGFP-expressing pyramidal neurons were observed in the superior temporal sulcus and other cortical areas, consistent with previous reports using other retrograde tracers. The region within the rectangle is re-photographed at higher magnification in (C). Darkened area (arrow) corresponds to the fringe of the injection site. (C) EGFP-expressing neurons in layers 3 and 5 in the lower bank of the superior temporal sulcus. Scale bars = 1.0 cm in B, 0.5 mm in C.

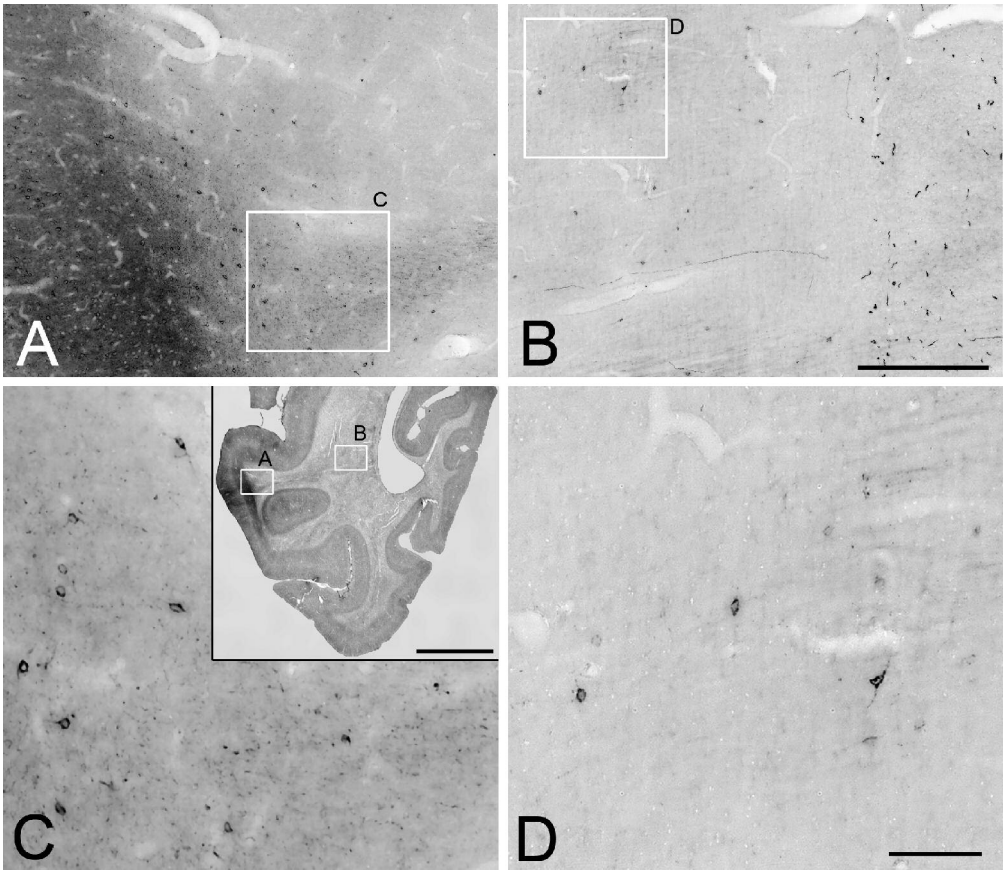

Figure 2 Photomicrographs showing retrogradely labeled neurons in the white matter (putative non-pyramidal neurons) after an injection of CTB-Alexa488 in area V4. (A) A portion of the injection site (at left) and scattered neurons in the subjacent white matter. This field is higher magnification of the boxed □“A□” region, from the histological section inset in (C). (B) Scattered neurons are labeled in the medial white matter. This field is higher magnification of the boxed □“B” region from the histological section (inset in (C). Short fragments of BDA-labeled fibers (labeled by an injection of BDA in area V1) are evident further medially, at right. (C) Higher magnification of labeled neurons below the injection site (from the boxed □“C□” region in (A)). Inset is low magnification of a coronal histology section, showing the anterior edge of the injection site and the location of the two fields shown with labeled cells. (D) Higher magnification of labeled neurons from the medial location, at the □“D□” box in (B). Scale bars= 500 μm in B (for A and B), 50 μm in D (for C and D), 5 mm in the inset.

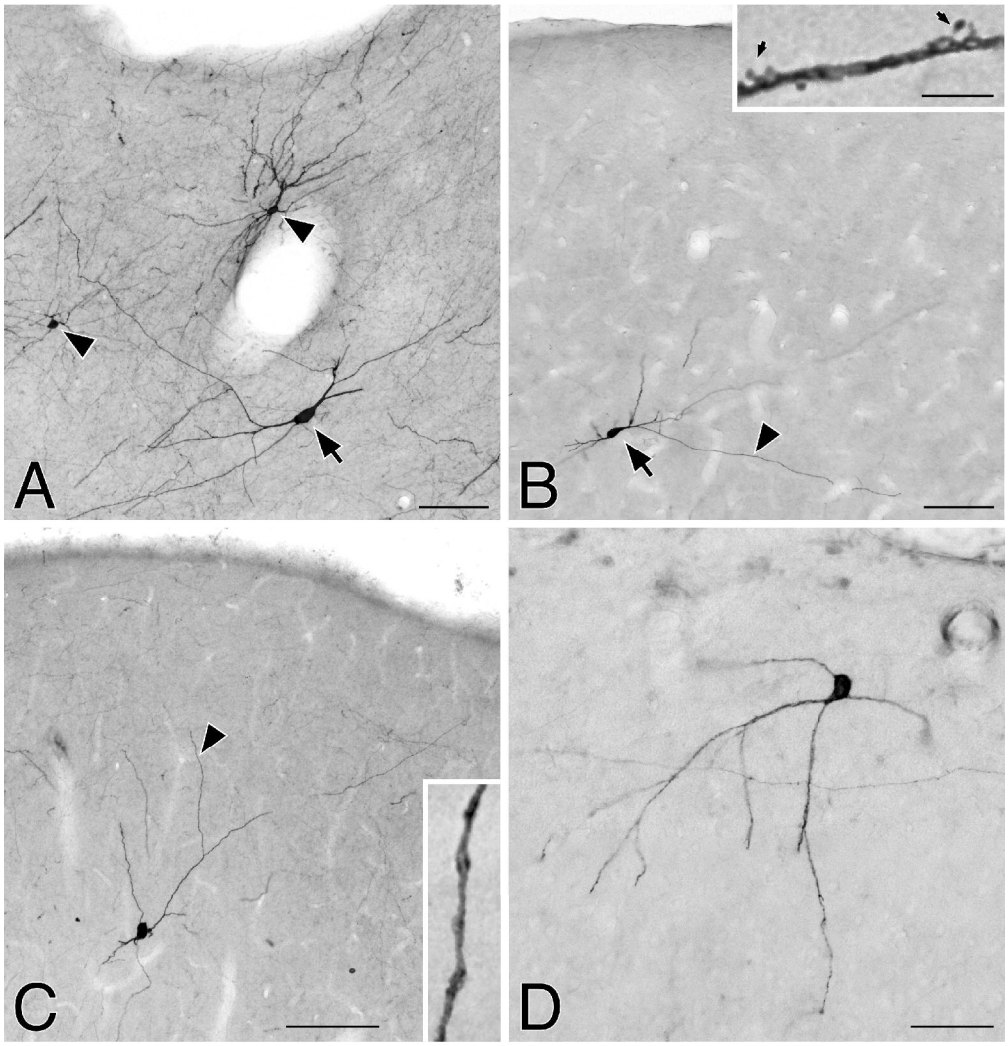

Figure 3 Photomicrographs showing retrogradely labeled non-pyramidal neurons in the gray matter after injections of AdSynEGFP. (A) Neuron in layer 3 (arrow) of the depth of the superior temporal sulcus (STS; section 91 in Fig. 4) after an injection in area TEO (case R116). Two adjacent pyramidal neurons are evident (arrowheads). (B) Another neuron in layer 3 (arrow) of the lower bank of the STS (section 62 in Fig. 4), in case R116. Dendrites are sparsely spinous (see arrows in higher magnification inset, which is from the region at arrowhead in (B)). (C) Neuron in layer 3 of the lower bank of the STS, in case 135 (injection in posterior TE). (D) Neuron at the border of layers 1 and 2 in area V2, after the injection in V1 (Fig. 5). Scale bars = 100 μm in A-D, 5 μm in the inset (C same as in B).

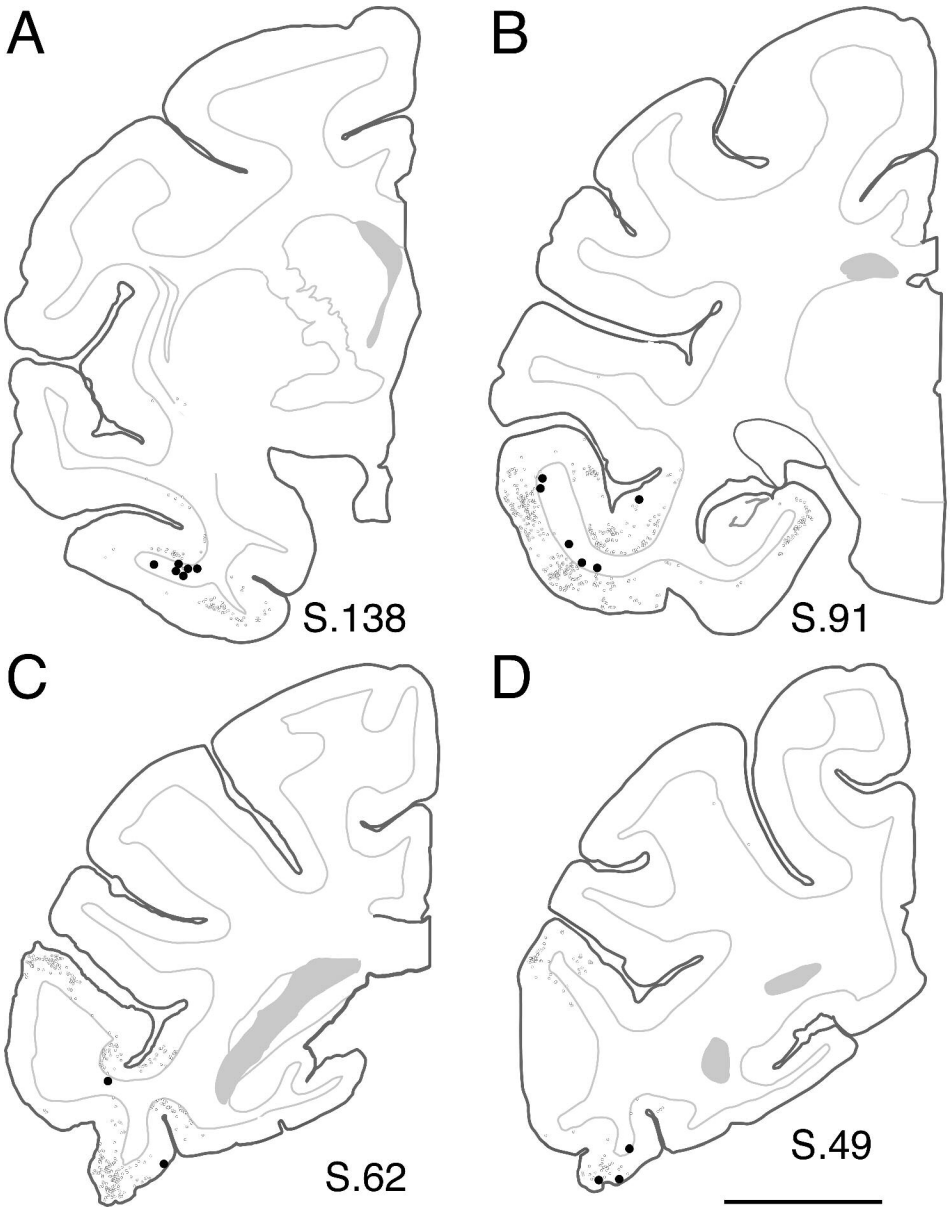

Figure 4 (A-D) Coronal section outlines from four AP levels in case R116 (injection of AdSynEGFP in area TEO), where medial is at the right. Numbers indicate AP progression, where smaller numbers are more posterior. Dots represent EGFP-expressing neurons, pyramidal (small dots) and non-pyramidal (large dots), where one dot = one neuron. Shaded regions = lateral ventricle. Scale bar = 1.0 cm.

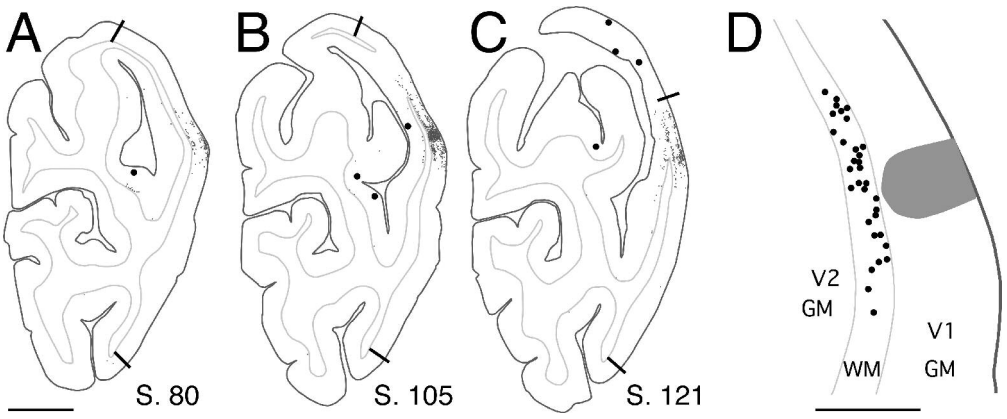

Figure 5 (A-C) Three coronal section outlines illustrating the distribution of non-pyramidal neurons in the gray matter, in areas V2 and V3 after the injection in area V1. Smaller numbers are more posterior, large dots = non-pyramidal neurons and small dots = pyramidal neurons. For simplicity, only non-pyramidal neurons are shown in V2 and V3. Short lines denote V1/V2 borders on the lateral surface. The peri-injection zone is at section 105. (D) A higher magnification view at right shows the distribution of white matter neurons in the immediate vicinity of the injection (shaded portion; section 107). There was no invasion of the white matter, either by injection needle or halo. Scale bar = 5 mm in A-C, 1 mm in D.

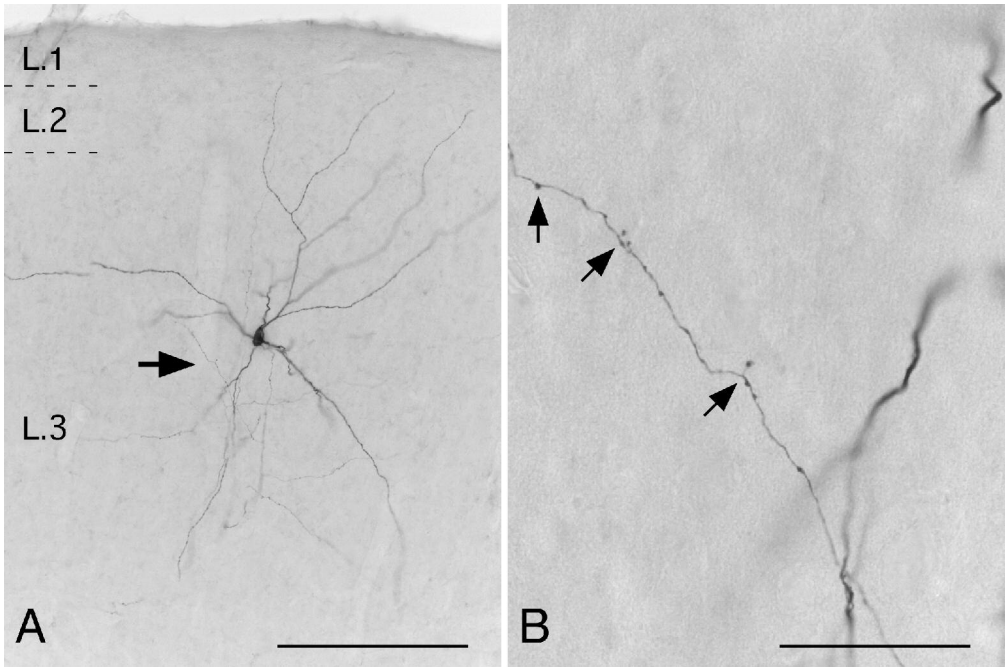

Figure 6 Axonal boutons are sparsely distributed in the proximal portion. (A) Non-pyramidal neuron in layer 3 of area V3 (section 105, Fig. 5). Arrow indicates axon. (B) Higher magnification from the arrow in (A). Terminal specializations are both beaded (upper arrow) and stalked (bottom two arrows). Scale bars = 200 μm in A, 40 μm in B.

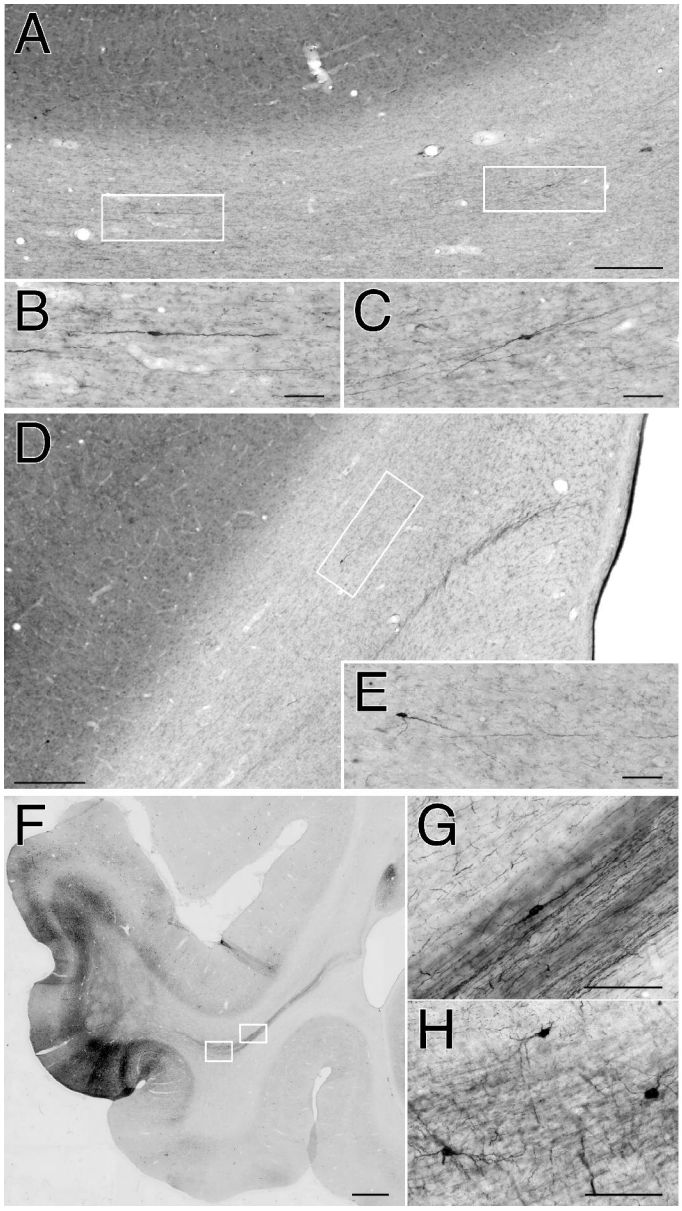

Figure 7 Photomicrographs showing retrogradely labeled non-pyramidal neurons in the white matter after injections of AdSynEGFP. (A- E) Retrogradely labeled neurons at two AP levels from case 313 (injection in area TEp; A and D are from below the STS, about 3.0 mm apart). White matter neurons, as shown here, tend to have a narrow, compressed dendritic field, in contrast with the larger dendritic field of neurons in the gray matter (compare Fig. 2). Rectangles in (A) and (D) are re-photographed at higher magnification in (B), (C), and (E). (F) Several neurons are evident in the white matter, situated in a bundle of labeled axons issuing from the vicinity of the injection site (case 135). (G, H) Higher magnification from the rectangles in (F). Scale bars = 500 μm in A, D; 100 μm in B, C, E; 1.0 mm in F; 200 μm in G, H.

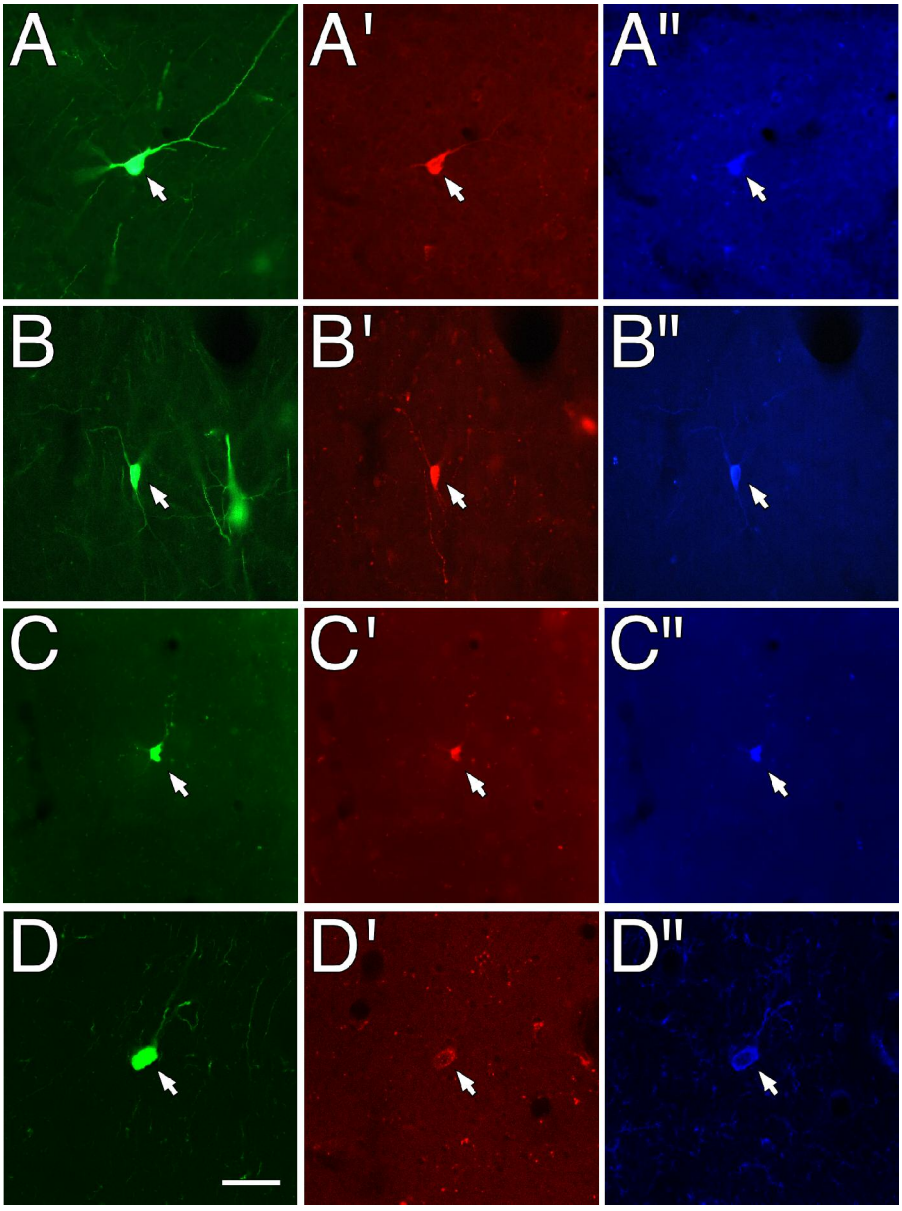

Figure 8 Fluorescent photomicrographs showing neurochemical characterization of EGFP-labeled non-pyramidal neurons. (A) EGFP-expressing non-pyramidal neuron (arrow) in the white matter (injection of AdSynEGFP in TEO, case R116). This is co-labeled with somatostatin (A□ ❟) and GAD67 (A□ ❟❟). (B) EGFP-expressing non-pyramidal neuron (arrow) in layer 3 (from section 91, Fig. 4). This is co-labeled with somatostatin (B□ ❟) and nNOS (B□ ❟❟). (C) EGFP-expressing non-pyramidal neuron (arrow) in the white matter, is positive for somatostatin (C ❟) and calretinin (C ❟❟). (D) EGFP-expressing neuron (arrow) in the white matter, positive for somatostatin (D□ ❟) and m2 muscarinic receptor (D□ ❟❟). Scale bars = 50 μm.

TABLE1. Antibodies Used.

Antibody	Source	Catalog No. (Lot No.)	Type	Immunogen	Species	Dilution
GAD67	Chemicon	MAB5406 (25080061)	Monoclonal IgG2a	recombinant GAD67	Mouse	1/400
Parvalbumin	SWANT	PV-28 (5.5)	Polyclonal antiserum	parvalbumin from rat muscle	Rabbit	1/400
Somatostatin	Chemicon	MAB354 (0602021758)	Monoclonal IgG2b	synthetic somatostatin	Rat	1/400
Calretinin	SWANT	7699/4 (18299)	Polyclonal antiserum	recombinant calretinin	Rabbit	1/1000
nNOS	Chemicon	AB1632 (23031420)	Affinity purified polyclonal antibody	synthetic peptide of nNOS	Rabbit	1/400
m2	Chemicon	AB5166 (21071386)	Affinity purified polyclonal antibody	recombinant human m2	Rabbit	1/400
EGFP	Tomioka and Rockland (2005)	-	Affinity purified polyclonal antibody	recombinant EGFP	Guinea Pig	1/500*
EGFP	Tomioka and Rockland (2005)	-	Affinity purified polyclonal antibody	recombinant EGFP	Rabbit	1/500*
Alexa488	Invitrogen	A-11094 (48619A)	Polyclonal IgG	synthetic Alexa Fluor 488	Rabbit	1/1000

* Antibodies to EGFP were diluted to be 1 µg/ml for immunocytochemistry.

Table 2: Morphometric properties of retrogradely labeled non-pyramidal neurons

Layer (total number of neurons)	Number of analyzed neurons	Average soma size (μm^2)	soma size (μm^2) (minimum – maximum)
L.1 (n = 1)	1	150	—
L.2 (n = 9)	7	151	128 – 168
L.3 (n = 31)	27	210	125 – 431
L.4 (n = 0)	0	—	—
L.5 (n = 5)	4	205	182 – 231
L.6 (n = 5)	3	189	170 – 211
WM (n = 269)	179	159	87 – 285

— no data.

Table 3: Neurochemical characterization of EGFP-expressing non-pyramidal neurons

NEURONS						
	GAD67	PV	SS	CR	nNOS	m_2
$GAD67^+$ $EGFP^+$	—	0% (0/21)	90.0% (74/82)	13.9 %(5/36)	—	—
SS^+ $EGFP^+$	93.7% (74/79)	—	—	23.3% (7/30)	94.1% (16/17)	95.2% (20/21)

— not screened.